Journal of Anatomy

J. Anat. (2010) **217**, pp624–630 doi: 10.1111/j.1469-7580.2010.01285.x

Stereological assessment of pancreatic beta-cell mass development in male Zucker Diabetic Fatty (ZDF) rats: correlation with pancreatic beta-cell function

Sarah Juel Paulsen,[1,2,3] Niels Vrang,[1,3] Leif Kongskov Larsen,[1] Philip Just Larsen[1] and Jacob Jelsing[1,3]

[1]*Rheoscience A/S, Roedovre, Denmark*
[2]*BMB, University of Southern Denmark, Odense M, Denmark*
[3]*Gubra, Frederiksberg C, Denmark*

Abstract

The present study was initiated to improve our understanding of pancreatic beta-cell dynamics in male Zucker Diabetic Fatty (ZDF) rats and hence provide a framework for future diabetes studies in this animal model. Male ZDF rats from 6, 8, 10, 12, 14, 16, 20 and 26 weeks of age were subjected to an oral glucose tolerance test (OGTT). The animals were then euthanized and pancreases were removed for morphometric analyses of pancreatic beta-cell mass. As evident by a marked fourfold increase in insulin secretion, insulin resistance developed rapidly from 6 to 8 weeks of age. Simultaneously, the pancreatic beta-cell mass expanded from 6.17 ± 0.41 mg at 6 weeks of age, reaching a maximum of 16.5 ± 2.5 mg at 16 weeks of age, at which time pancreatic beta-cell mass gradually declined. The corresponding changes in glucose/insulin homeostasis were analysed using a standard insulin sensitivity index (ISI), an area under the curve (AUC) glucose-insulin index, or simple semi-fasted glucose levels. The study demonstrated that male ZDF rats underwent rapid changes in pancreatic beta-cell mass from the onset of insulin resistance to frank diabetes coupled directly to marked alterations in glucose/insulin homeostasis. The study underscores the need for a critical co-examination of glucose homeostatic parameters in studies investigating the effects of novel anti-diabetic compounds on pancreatic beta-cell mass in the male ZDF rat. A simple assessment of fasting glucose levels coupled with information about age can provide a correct indication of the actual pancreatic beta-cell mass and the physiological state of the animal.

Key words pancreatic beta-cell mass development; stereology; Zucker Diabetic Fatty rat.

Introduction

An increasing number of antidiabetic therapies with potential anti-apoptotic and/or proliferative effects at the pancreatic beta-cell level are currently being actively pursued (Holst, 2007; Holst et al. 2008). However, as pancreatic beta-cell mass can not be visualized directly in the intact organism, the only way to determine pancreatic beta-cell mass is by post-mortem histological analysis. Despite the existence of well-described quantitative methods for accurate and reliable determination of pancreatic beta-cell mass, many reports of pancreatic beta-cell mass are still influenced by sample-bias or are of a purely descriptive nature, making firm conclusions difficult.

Correspondence
Jacob Jelsing, Gubra ApS, Ridebanevej 12, 1870 Frederiksberg, Denmark. T: + 45 31522652; E: jacob@gubra.dk

Accepted for publication *16 July 2010*
Article published online *30 August 2010*

Furthermore, it is well-known that one of the most widely used animal models of type II diabetes, the male Zucker Diabetic Fatty rat (ZDF-rat), undergoes rapid changes in pancreatic beta-cell mass which further warrants for careful interpretation of results (Lee et al. 1994; Hirose et al. 1996; Pick et al. 1998; Janssen et al. 1999, 2001; Etgen & Oldham, 2000; Finegood et al. 2001; Griffen et al. 2001; Schmidt et al. 2003; Goh et al. 2007; Topp et al. 2007).

The male ZDF rat progresses rapidly from insulin resistance into frank diabetes within a couple of weeks (Chen & Wang, 2005). The ZDF rat was originally generated from the Zucker Fatty (ZF) rat line through selective inbreeding of the animals with the highest blood sugars (Peterson et al. 1990). Like the obese Zucker fatty (*fa/fa*) rat, the ZDF rat is obese, hyperphagic and hypometabolic due to a genetic defect in the leptin receptor (Topp et al. 2007). However, unlike the obese Zucker rat, the ZDF rat is unable to compensate for the obesity-linked insulin resistance by continuously increasing pancreatic beta-cell mass and insulin production (Griffen et al. 2001; Topp et al. 2007).

Male ZDF rats spontaneously develop diabetes, whereas female ZDF rats only do so when fed a high fat diet (Janssen et al. 1999).

Despite the frequent use of ZDF rats in studies of pancreatic beta-cell modulation, a thorough study of the temporal course of pancreatic beta-cell mass and pancreatic beta-cell function has not yet been performed. Previous studies of pancreatic beta-cell mass dynamics in both male (Pick et al. 1998; Finegood et al. 2001; Topp et al. 2007) and female (Topp et al. 2007) ZDF rats have only included rats up to 16 weeks of age and none of these studies has used glucose tolerance tests to characterize the individual glucose homeostasis or insulin secretion capacity. The present study was initiated to fully characterize and investigate the correlation between stereological estimates of pancreatic beta-cell mass and the development of glucose intolerance and insulin resistance in male ZDF rats. To date, an inadequate knowledge about the development of diabetes in the male ZDF rat hampers the interpretation of data in intervention studies, and leaves plenty of room for speculations rather than firm conclusions.

Materials and methods

Animals

All experiments were conducted in accordance with internationally accepted principles for the care and use of laboratory animals and were approved by the Danish committee for animal research. Studies were carried out in male ZDF rats acquired at the age of 5 weeks from Charles River, USA. Animals were housed individually and kept on a 12-h light, 12-h dark cycle (lights on at 6 AM) in a temperature-controlled environment (22–24 °C), with *ad libitum* access to Purina 5008 diet and water.

Animal groups

Following acclimatization, animals were randomized into eight groups according to body weight (n = 9 per group, mean body weight ± SEM: 150 ± 0.2 g). The groups were terminated at 6, 10, 12, 14, 16, 20 and 26 weeks of age.

Oral glucose tolerant test

Three days prior to termination, rats were subjected to an OGTT. The test was carried out at 08.00 hours. The day before the test, animals were offered 50% of their average 24-h food intake measured during the week before termination. Blood samples were taken from a tail vein at −15, 0, 15, 30, 60, 120 and 240 min after oral administration of 1 g kg^{-1} glucose (glucose 500 mg mL^{-1}; Fresenius Kabi, Sweden). The oral glucose load was given as gavage via a gastric tube connected to a syringe to ensure accurate dosing. Prior to the OGTT, animals were handled to accustom them to the experimental procedure. No anaesthesia was given prior to or during the OGTT. Plasma glucose was measured using a VITROS 250 Chemistry System (Ortho-Clinical Diagnostics, Johnson and Johnson). Plasma insulin samples were measured in duplicate using an ultra-sensitive ELISA method (Diamyd Diagnostics, Sweden; sensitivity 0.13 μg L^{-1}, inter- and intra-assay specificity within 4–5%).

Termination

At the day of termination, body weights were recorded and the rats were killed by CO_2 anaesthesia and subsequent decapitation. Trunk blood was collected for analysis of fed levels of triacylglycerol (TG), cholesterol, glucose and non-esterified fatty acids (NEFA). Immediately hereafter, the pancreas was removed *en-bloc* with liver and gut and transferred to 4% paraformaldehyde dissolved in phosphate-buffered saline (50 mM, pH 7.4). The tissue was stored in 4% paraformaldehyde until further processing (see below). Plasma TG, cholesterol and glucose were analyzed using a VITROS 250 Chemistry System. NEFA was determined using a colorimetric kit (NEFA-C; WAKO Chemicals, Osaka, Japan; sensitivity 0.0014 mEq L^{-1}).

Pancreas histology

The paraformaldehyde-fixed pancreases were carefully dissected and weighed. The tissue was then rolled into a cylinder, dehydrated in ethanol and xylene series, before infiltration overnight in paraffin (Fig. 1). The infiltrated cylinder was cut transversely into 2–3-mm-thick slabs using a systematic slicer with a random starting position within the first slab thickness. The resulting 8–10 slabs were embedded on their cut surfaces in blocks of paraffin (Fig. 1). A single 5-μm top section from each block was cut and arranged on two to three object slides repre-

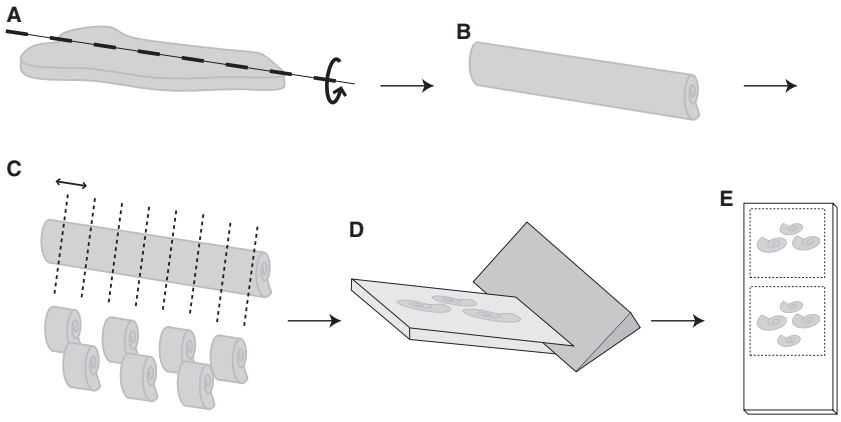

Fig. 1 Schematic illustration of sampling principles. The formalin fixated pancreas was dissected (A), rolled into a cylinder (B) and infiltrated in paraffin. The cylinder was cut transversely into systematic, uniform, random slabs (C). Each slab was embedded in blocks of paraffin (two per block) and a single top section from each block was then obtained (D). Sections were arranged two-and-two on object glasses (E) and finally stained for insulin-immunoreactivity.

senting in total a systematic uniform random sample of the whole pancreas (Fig. 1). Slides were subsequently subjected to immunohistochemistry for insulin. The sections were deparaffinized in xylene and rehydrated with decreasing ethanol solutions to water. Antigen retrieval was performed by placing the sections in 10 mM citrate buffer, pH 6, at 90 °C for 15 min. Endogenous peroxidase was blocked by 1% H_2O_2 in potassium containing phosphate-buffered saline, followed by blocking in 10% rabbit normal serum (Dakocytomation X0902). Pancreatic beta-cells were stained using guinea-pig anti-insulin (Dakocytomation A0564), followed by horseradish peroxidase-coupled rabbit anti-guinea pig (Dakocytomation P0141) and developed in NovaRed (Vector Laboratories SK4800). Finally, slides were counterstained with Mayer's haematoxylin and mounted with Pertex Mounting Media.

Stereological estimation of pancreatic beta-cell mass and fat infiltration

The stereological estimation of pancreatic beta-cell mass was carried out by an observer blinded to the experimental groups. Pancreatic beta-cell mass was estimated by point counting using a grid system on an on-screen magnification of approximately ×550. Sections were scanned in a random systematic way by use of the new CAST system (Visiopharm, Denmark) to control the stage and the data collection. All points hitting the structure of interest were counted. A three-point grid per frame was used for the estimation of pancreas mass, with the pancreatic beta-cell mass being estimated using a denser grid to assure the accumulation of roughly equal number of 'hits' per tissue element. Similarly, the grid system was used to correct for the presence of non-pancreatic elements (i.e. lymph and fat tissue) in the dissected sample. The density of the grid system was designed and optimized in a preliminary pilot study using the CE prediction formula for the Cavalieri estimator (Gundersen et al. 1999). In general, the grid system was considered optimal when 100–250 points, distributed on 8–10 sections, were hitting the structures of interest.

The number of points hitting the structure of interest was finally converted into mass by multiplying the area fraction with dissected pancreas mass, taking the grid ratio into consideration (Bock et al. 2003).

Calculation of the insulin sensitivity index

The insulin sensitivity index (ISI) was calculated according to Matsuda & DeFronzo (1999) as:

$$\mathrm{ISI} = \frac{10000}{\sqrt{(\mathrm{FPG} \times \mathrm{FPI}) \times (\mathrm{AUC\_OGTTglucose} \times \mathrm{AUC\_OGTTinsulin})}}$$

where FPG under the curve and FPI represent fasting plasma glucose and insulin, respectively (t_{-15}). Area (AUC) OGTTglucose and OGTTinsulin are the AUC glucose or insulin values respectively obtained during the OGTT (modification from Matsuda & DeFronzo, 1999). AUC OGTT values are calculated from −15, 0, 15, 30, 60, 120, 180 and 240 min after glucose load.

Statistics

Statistical analyses were performed using STATVIEW 4.57 software. All parameters were compared by one-way analysis of variance (ANOVA) followed by Fisher's *post-hoc* analysis. Results are presented as mean ± SEM.

Results

Oral glucose tolerance test

OGTT glucose and insulin data from all animal groups are shown in Fig. 2. Both semi-fasted glucose levels (t_{-15} values) and fed glucose levels increase with age, whereas glucose tolerance deteriorates with age (Table 1, Fig. 2A,C). At 6 weeks of age, ZDF rats are able to handle an oral glucose load with a relatively low level of insulin secretion (Fig. 2B,D). At 8 weeks of age, a marked increase in insulin secretion is nearly sufficient to maintain normoglycaemia during the OGTT, but from 10 weeks and onwards, the insulin secretory capacity deteriorates (Fig. 2B,D).

Bodyweight and terminal blood biochemistry

Bodyweights are shown in Table 1. Following an initial rapid growth phase, bodyweight was observed to plateau around week 14, coinciding with a pronounced deterioration in glucose tolerance (Fig. 2A). From week 14 and onwards, bodyweight remained stable.

Blood samples obtained at the time of termination were used for determination of fed glucose, NEFA, TG and cholesterol levels and all demonstrated a steady increase from 6 to 26 weeks of age (Table 1).

Stereological determination of pancreatic beta-cell mass

Insulin-immunoreactivity was used to phenotypically characterize and discriminate pancreatic beta-cells from counterstained adjacent insulin-negative endocrine (alpha-, delta- and gamma cells) and exocrine cells. Although differences were apparent, the procedure in general gave rise to well defined islets with clearly stained and easily distinguishable pancreatic beta-cells (Fig. 3). The quantitative estimation of pancreatic beta-cell mass demonstrated that pancreatic beta-cell mass increased from 6.2 ± 0.4 mg at 6 weeks of age to 16.5 ± 2.8 mg at 16 weeks of age (Fig. 4). After this, the average pancreatic beta-cell mass started to decline, reaching a mean of only 7.1 ± 0.7 mg at week 26 (Fig. 4). Pancreatic beta-cell mass per bodyweight remained constant from 6 to 16 weeks of age (mean week 6–16: 36.4 ± 1.5 mg kg^{-1}) followed by a statistically significant reduction to week 20 (23.0 ± 2.0 mg kg^{-1}) to week 26 (16.8 ± 1.0 mg kg^{-1}). The change in pancreatic beta-cell mass can be coupled with clear qualitative differences in overall cytology, with islets appearing small and well defined at 6–8 weeks of age (Fig. 3A) and a clear deterioration of normal islet structure and insulin-immunoreactivity at later stages (Fig. 3B,C). In ZDF rats 20–26 weeks old,

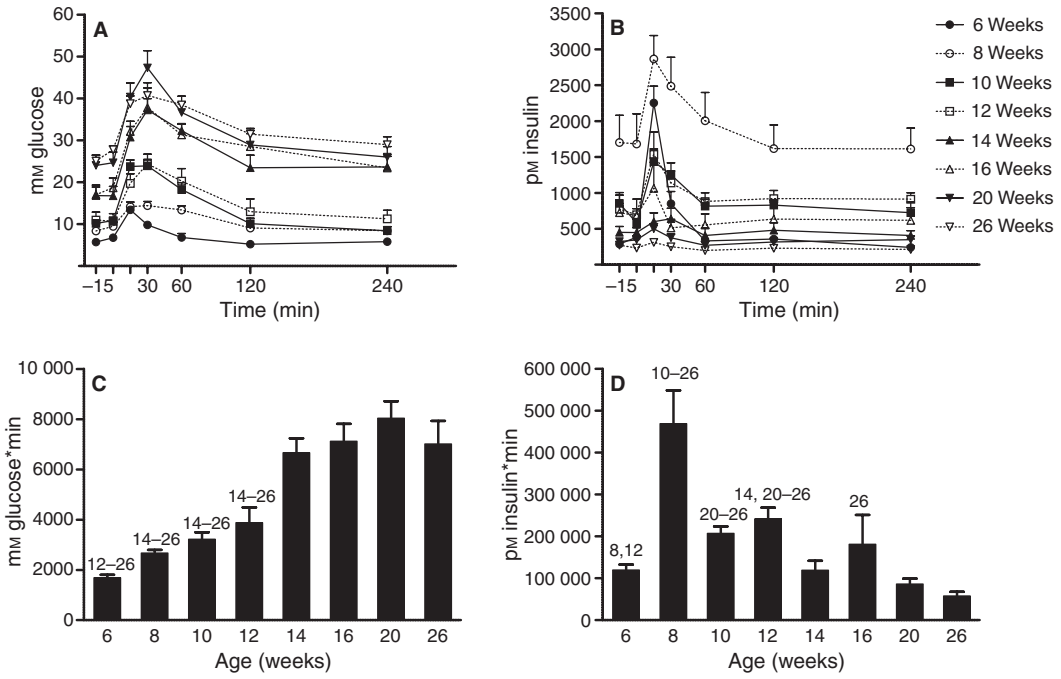

Fig. 2 Oral glucose tolerance test in male Zucker diabetic fatty rats carried out at 6, 8, 10, 12, 14, 16, 20 and 26 weeks of age. Plasma glucose (A) and plasma insulin (B) levels are shown from 15 min prior to 240 min after administration of the glucose load. Integrated areas under the curve (AUC) are shown for both glucose (C) and insulin (D). Glucose and insulin AUC data were compared by one-way analysis of variance (ANOVA) followed by Fisher's *post-hoc* analysis. Statistically significant differences ($P \leq 0.05$) between time points are shown as numbers (corresponding to age in weeks) above relevant bar graphs. Results are presented as mean ± SEM. $n = 9$.

Table 1 Body weights and blood analytes measured during an oral glucose tolerance tests. Body weights measured prior to initiation of semi-fasting. Pancreas weight at termination adjusted for non-pancreatic tissue elements. Semi-fasted insulin and glucose values were measured 15 min prior to glucose loading. Fed glucose, NEFA, cholesterol and triglyceride levels were measured at termination.

Age (weeks)	Body weight (g)	Pancreas weight (g)	Insulin – fasted (pM)	Glucose – fasted (mM)	Glucose – fed (mM)	NEFA – fed (mEq L^{-1})	Chol – fed (mM)	TG – fed (mM)
6	$183.4 \pm 5.7^{8–26}$	$0.70 \pm 0.02^{8–26}$	$286 \pm 47^{8–10}$	$5.7 \pm 0.2^{12–26}$	$8.2 \pm 0.3^{12–26}$	$0.25 \pm 0.03^{14–26}$	$3.5 \pm 0.2^{14–26}$	$2.0 \pm 0.1^{8–26}$
8	$276.6 \pm 5.8^{10–26}$	$0.88 \pm 0.03^{16,26}$	$1701 \pm 380^{10–26}$	$8.4 \pm 0.3^{14–26}$	$9.8 \pm 0.9^{12–26}$	$0.30 \pm 0.03^{14–26}$	$3.6 \pm 0.1^{14–26}$	5.3 ± 0.5
10	$337.2 \pm 6.8^{12–26}$	0.97 ± 0.04^{26}	854 ± 117	$10.2 \pm 0.6^{14–26}$	$14.5 \pm 2.9^{14–26}$	$0.34 \pm 0.03^{14–26}$	$3.3 \pm 0.1^{12–26}$	6.1 ± 0.6
12	395.5 ± 11.8	$0.88 \pm 0.03^{16,26}$	772 ± 81	$11.0 \pm 1.9^{14–26}$	$18.5 \pm 3.5^{14–26}$	$0.39 \pm 0.05^{14–26}$	$4.3 \pm 0.1^{16–26}$	6.4 ± 0.4
14	$378.0 \pm 11.3^{16,26}$	0.89 ± 0.04^{26}	449 ± 84	$16.8 \pm 2.0^{20–26}$	29.4 ± 2.2^{26}	0.62 ± 0.08^{26}	$4.9 \pm 0.2^{20–26}$	6.5 ± 0.8
16	411.3 ± 16.9	1.00 ± 0.04^{26}	725 ± 280	$17.0 \pm 2.3^{20–26}$	28.4 ± 1.9^{26}	0.70 ± 0.08^{26}	5.5 ± 0.3^{26}	5.5 ± 0.8
20	401.4 ± 10.1	0.94 ± 0.05^{26}	323 ± 46	25.7 ± 2.0	29.7 ± 2.6^{26}	0.60 ± 0.09^{26}	6.3 ± 0.4^{26}	5.3 ± 0.3
26	414.7 ± 20.1	1.17 ± 0.05	448 ± 180	25.1 ± 1.4	58.0 ± 0.1	1.00 ± 0.33	9.6 ± 0.7	5.6 ± 0.3

NEFA, non-esterified fatty acids; Chol, cholesterol; TG, triacylglycerol.
Values are presented as group average ± SEM. Data with numbers in superscripts (referring to groups by age) differ from each other by $P \leq 0.05$.

a large number of fat cells were observed infiltrating the exocrine tissue (Fig. 3D).

Relationship between pancreatic beta-cell mass and plasma glucose and insulin levels

As the insulin sensitivity declines rapidly from 6 to 8 weeks of age (Fig. 5A), the insulin sensitivity index (ISI) of Matsuda & DeFronzo (1999) is of little physiological importance in the ZDF rat model. As an alternative measure of the relationship between insulin secretory capacity and glucose handling, we used a simple AUC-glucose-insulin index derived from the relationship between AUC glucose and AUC insulin. Using this measure it was demonstrated that the AUC-glucose-insulin index steadily increases from 8 to 26 weeks of age (Fig. 5B). As an alternative indicator of the

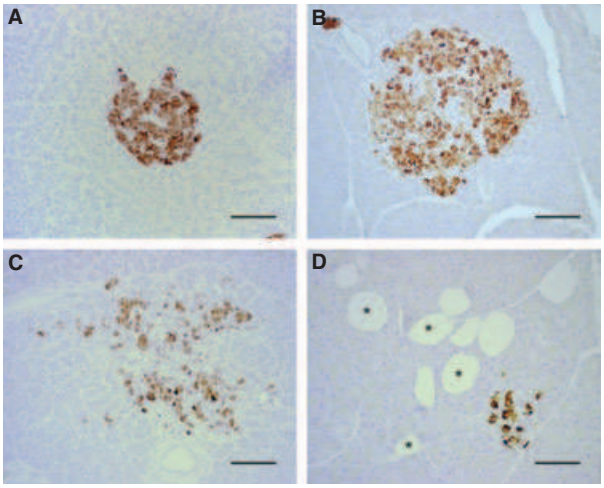

Fig. 3 Pancreatic islet morphology of -8 (A), 12- (B), 16- (C) and 26-day-old (D) male Zucker diabetic fatty rats as shown by immunoperoxidase (brown) staining for insulin immunoreactivity. Islet size appears to be larger in 12-week-old rats (B) when compared with 8-week-old rats (A). At 16 weeks of age the islet shape is highly irregular, with weakly stained pancreatic beta-cells (C). At 20 (not shown) and 26 weeks of age (D) islets in general appeared small, with a high number of fat cells seen infiltrating the exocrine pancreas. Asterisks denote fat cells. Scale bar: 100 μm.

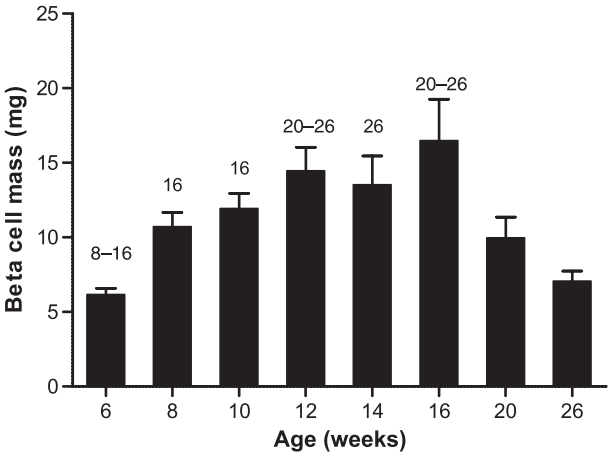

Fig. 4 Stereological assessment of pancreatic beta-cell mass in male ZDF rats. Rats were terminated 3 days after an oral glucose tolerance test. Differences in pancreatic beta-cell mass between time points were compared by one-way analysis of variance (ANOVA) followed by Fisher's *post-hoc* analysis. Statistically significant differences ($P \leq 0.05$) between time points are shown as numbers (corresponding to age in weeks) above relevant bar graphs. Results are presented as mean pancreatic beta-cell mass ± SEM. $n = 9$.

relationship between insulin secretory capacity and glucose handling we then assessed semi-fasted glucose levels as an easy, noninvasive way to monitor the diabetic status of ZDF rats in relation to age. As seen for the AUC-glucose-insulin index, this simple measure demonstrates a similar constant increase throughout the study period (Fig. 5C).

To correlate changes in pancreatic beta-cell mass with overall glucose control, the semi-fasted glucose levels were plotted as a function of individual pancreatic beta-cell mass, illustrating the relationship of pancreatic beta-cell mass and glucose levels as they occur in the ZDF rat (Fig. 5D). It is evident that in young rats (6–12 weeks of age) semi-fasted glucose levels remain relatively stable, apparently because of an ability to increase pancreatic beta-cells mass. However, at 14–16 weeks of age and onwards, pancreatic beta-cell mass starts to decline. Although in a few rats the pancreatic beta-cell mass seems to keep increasing, the general tendency demonstrates a decreasing pancreatic beta-cell mass coincident with a parallel increase in the semi-fasted glucose levels.

Discussion

The development of diabetes in the male ZDF rat is well described (Lee et al. 1994; Hirose et al. 1996; Pick et al. 1998; Janssen et al. 1999, 2001; Etgen & Oldham, 2000; Finegood et al. 2001; Griffen et al. 2001; Schmidt et al. 2003; Goh et al. 2007; Topp et al. 2007). Similarly, a number of studies have dealt with pancreatic beta-cell mass dynamics in both male (Pick et al. 1998; Finegood et al. 2001; Topp et al. 2007) and female (Topp et al. 2007) ZDF rats demonstrating both secretory defects in the prediabetic state (Pick et al. 1998) as well as disruption of normal islet architecture, pancreatic beta-cell degranulation and increased pancreatic beta-cell death (Janssen et al. 2001) during the progression of diabetes. However, none of these studies has examined rats older than 16 weeks of age or used glucose tolerance tests to characterize the individual glucose homeostasis or insulin secretory capacity. Furthermore, the current study is the first to apply stereological sampling in combination with point-counting (Gundersen & Jensen, 1987) in the ZDF rat pancreas to avoid sampling bias and to give a reliable and precise estimate of islet fractions. In this respect, however, it should be noted that pancreatic beta-cells were identified based on their insulin-immunoreactivity and that the functional state of the pancreatic beta-cells may affect cell surface antigen specificity.

To obtain a better insight into the correlation between pancreatic beta-cell mass, glucose homeostasis and insulin sensitivity, we initially intended to use the insulin sensitivity by Matsuda and DeFronzo (Matsuda et al. 1999) as a marker of diabetic status. Using this index, we demonstrated a dramatic drop in ISI between 6 and 8 weeks of age which pointed to a rapid development of insulin resistance in the ZDF rat (Etgen & Oldham, 2000). However, from 8 to 26 weeks of age, the area under the insulin and glucose curves declined and increased, respectively, leading to a low and stable ISI at all time points, making these curves unsuitable descriptors of the relationship between insulin secretory capacity and glucose handling in this animal model. Instead, we evaluated the use of an OGTT AUC-glucose-

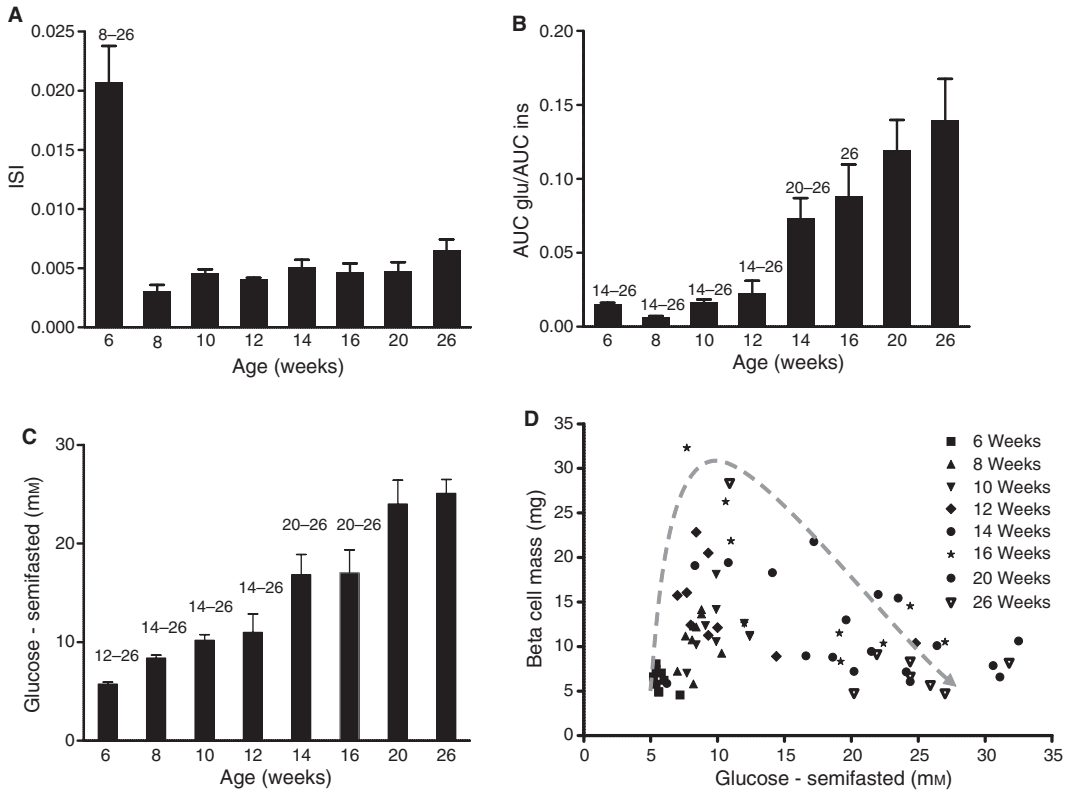

Fig. 5 Plasma insulin/glucose as a function of time and pancreatic beta-cell mass. (A) ISI, (B) AUC-glucose-insulin index, and (C) semi-fasted glucose levels in ZDF rats from 6 to 26 weeks of age. (D) Semi-fasted glucose vs. pancreatic beta-cell mass for all animals. The grey dashed tendency line in (D) depicts the pancreatic beta-cell mass changes in the male Zucker diabetic fatty rat. Initially, pancreatic beta-cell mass increases to compensate for the increased insulin demand, keeping the semi-fasted glucose low – but eventually pancreatic beta-cell mass starts to decline, leading to an increase in the glucose levels. ISI, AUC-glucose-insulin index and semi-fasted glucose levels were compared by one-way analysis of variance (ANOVA) followed by Fisher's *post-hoc* analysis. Statistically significant differences ($P \leq 0.05$) between time points are shown as numbers (corresponding to age in weeks) above relevant bar graphs. Results are presented as mean ± SEM. $n = 9$.

insulin index in addition to a simple, time-efficient and less stressful measurement of semi-fasted glucose only. We demonstrate that semi-fasted glucose levels in the ZDF rat increase from 8 to 26 weeks of age and that this measure separates the different age groups better than any other available parameter (AUC glucose, AUC insulin, fasting insulin, free fed glucose or free-fed insulin). More importantly, when plotted against corresponding estimates of pancreatic beta-cell mass, semi-fasted glucose clearly depicts important individual differences. In young animals, an increasing pancreatic beta-cell mass seems to be able to compensate for the increased insulin demand, keeping fasting glucose low. In contrast, individual pancreatic beta-cell mass starts to decline and the semi-fasted glucose level increases from 12 to 16 weeks of age. This opposing shift in parameters give rise to animals with very different glucose homeostasis even though pancreatic beta-cell mass is unchanged. Evidently, a simple read-out on changes in pancreatic beta-cell mass in pharmacological intervention studies may seriously hamper data interpretation. In addition, our data underscore that the time for termination should be carefully considered to clarify whether treatment leading to an apparent compound-mediated effect on pancreatic beta-cell mass represents an effect of increased pancreatic beta-cell proliferation and not simply prevention of the natural decline in beta cell mass. Finally, our data may be valid to provide a firm indication about the physiological state and individual pancreatic beta-cell mass simply by comparing age with the individual fasting glucose level.

The exact mechanism leading to pancreatic beta-cell mass expansion and decline was not pursued. However, the dramatic increase in plasma levels of free fatty acids and triglycerides from around 14 weeks of age (i.e. at the time when the most dramatic deterioration in glucose tolerance occurred consistent with a switch to fat metabolism) suggests that the pancreatic beta-cells experience both lipo- and glucotoxicity. Insulin-producing pancreatic beta-cells have previously been shown to be particularly sensitive to saturated fatty acids, as evidenced by several *in vitro* experiments in which chronic exposure of pancreatic beta-cells to fatty acids leads to decreased insulin secretion and subsequent apoptosis (Shimabukuro et al. 1998; Lupi et al. 2002; El-Assaad et al. 2003). Furthermore, long *in vitro* exposure to NEFA has been shown to reduce glucose- stimulated

insulin secretion in islets of both homozygous and heterozygous pre-diabetic ZDF rats to a greater extent than secretion in islets of control rats (Lee et al. 1994; Hirose et al. 1996).

Future studies will be valuable to understand the underlying molecular mechanism, for example, by assessing proliferation (Pick et al. 1998; Finegood et al. 2001), apoptosis (Pick et al. 1998), gluco- and lipotoxicity (Lee et al. 1994; Hirose et al. 1996; Shimabukuro et al. 1998; Lupi et al. 2002; El-Assaad et al. 2003), protein ubiquitination (Kaniuk et al. 2007; Kiraly et al. 2008) or genetic aspects (Griffen et al. 2001; Topp et al. 2007).

In conclusion, we have thoroughly characterized the development of diabetes in the male ZDF rat from 6 to 26 weeks of age by comparing changes in beta-cell mass with plasma levels of glucose and insulin. The data highlight the importance of comparing pancreatic beta-cell mass with concomitant semi-fasted glucose levels and provides a valuable baseline for depicting the individual pancreatic beta-cell status in ZDF rats simply by monitoring semi-fasting glucose levels as a non-invasive measure that can be obtained repeatedly and relatively easily during intervention studies. Recently, there has been a strong demand for reliable animal models predicting the protective or proliferative effects of pharmaceutical preparations on pancreatic beta-cells. We believe the present data provide crucial information for the continued use of the male ZDF rat as a valuable type-II diabetes animal model.

Acknowledgements

We thank Farida Sahebzadeh and Anna Maria Thomsen for excellent technical assistance.

References

Bock T, Pakkenberg B, Buschard K (2003) Increased islet volume but unchanged islet number in ob/ob mice. *Diabetes* **52**, 1716–1722.

Chen D, Wang MW (2005) Development and application of rodent models for type 2 diabetes. *Diabetes Obes Metab* **7**, 307–317.

El-Assaad W, Buteau J, Peyot ML, et al. (2003) Saturated fatty acids synergize with elevated glucose to cause pancreatic beta-cell death. *Endocrinology* **144**, 4154–4163.

Etgen GJ, Oldham BA (2000) Profiling of Zucker diabetic fatty rats in their progression to the overt diabetic state. *Metabolism* **49**, 684–688.

Finegood DT, McArthur MD, Kojwang D, et al. (2001) Beta-cell mass dynamics in Zucker diabetic fatty rats. Rosiglitazone prevents the rise in net cell death. *Diabetes* **50**, 1021–1029.

Goh TT, Mason TM, Gupta N, et al. (2007) Lipid-induced beta-cell dysfunction in vivo in models of progressive beta-cell failure. *Am J Physiol Endocrinol Metab* **292**, E549–E560.

Griffen SC, Wang J, German MS (2001) A genetic defect in β-cell gene expression segregates independently from the *fa* locus in the ZDF rat. *Diabetes* **50**, 63–68.

Gundersen HJ, Jensen EB (1987) The efficiency of systematic sampling in stereology and its prediction. *J Microsc* **147**, 229–263.

Gundersen HJ, Jensen EB, Kiêu K, et al. (1999) The efficiency of systematic sampling in stereology–reconsidered. *J Microsc* **193**, 199–211.

Hirose H, Lee YH, Inman LR, et al. (1996) Defective fatty acid-mediated beta-cell compensation in Zucker diabetic fatty rats. Pathogenic implications for obesity-dependent diabetes. *J Biol Chem* **271**, 5633–5637.

Holst JJ (2007) The physiology of glucagon-like peptide 1. *Physiol Rev* **87**, 1409–1439.

Holst JJ, Deacon CF, Vilsboll T, et al. (2008) Glucagon-like peptide-1, glucose homeostasis and diabetes. *Trends Mol Med* **14**, 161–168.

Janssen SW, Martens GJ, Sweep CG, et al. (1999) In Zucker diabetic fatty rats plasma leptin levels are correlated with plasma insulin levels rather than with body weight. *Horm Metab Res* **31**, 610–615.

Janssen SW, Hermus AR, Lange WP, et al. (2001) Progressive histopathological changes in pancreatic islets of Zucker Diabetic Fatty rats. *Exp Clin Endocrinol Diabetes* **109**, 273–282.

Kaniuk NA, Kiraly M, Bates H, et al. (2007) Ubiquitinated-protein aggregates form in pancreatic beta-cells during diabetes-induced oxidative stress and are regulated by autophagy. *Diabetes* **56**, 930–939.

Kiraly MA, Bates HE, Kaniuk NA, et al. (2008) Swim training prevents hyperglycemia in ZDF rats: mechanisms involved in the partial maintenance of beta-cell function. *Am J Physiol Endocrinol Metab* **294**, E271–E283.

Lee Y, Hirose H, Ohneda M, et al. (1994) Beta-cell lipotoxicity in the pathogenesis of non-insulin-dependent diabetes mellitus of obese rats: impairment in adipocyte-beta-cell relationships. *Proc Natl Acad Sci U S A* **91**, 10878–10882.

Lupi R, Dotta F, Marselli L, et al. (2002) Prolonged exposure to free fatty acids has cytostatic and pro-apoptotic effects on human pancreatic islets: evidence that beta-cell death is caspase mediated, partially dependent on ceramide pathway, and Bcl-2 regulated. *Diabetes* **51**, 1437–1442.

Matsuda M, DeFronzo RA (1999) Insulin sensitivity indices obtained from oral glucose tolerance testing: comparison with the euglycemic insulin clamp. *Diabetes Care* **22**, 1462–1470.

Matsuda M, Liu Y, Mahankali S, et al. (1999) Altered hypothalamic function in response to glucose ingestion in obese humans. *Diabetes* **48**, 1801–1806.

Peterson RG, Shaw WN, Neel M-A, et al. (1990) Zucker Diabetic Fatty Rat as a model for non-insulin-dependent diabetes mellitus. *ILAR News* **32**, 16–19.

Pick A, Clark J, Kubstrup C, et al. (1998) Role of apoptosis in failure of beta-cell mass compensation for insulin resistance and beta-cell defects in the male Zucker diabetic fatty rat. *Diabetes* **47**, 358–364.

Schmidt RE, Dorsey DA, Beaudet LN, et al. (2003) Analysis of the Zucker Diabetic Fatty (ZDF) type 2 diabetic rat model suggests a neurotrophic role for insulin/IGF-I in diabetic autonomic neuropathy. *Am J Pathol* **163**, 21–28.

Shimabukuro M, Zhou YT, Levi M, et al. (1998) Fatty acid-induced beta cell apoptosis: a link between obesity and diabetes. *Proc Natl Acad Sci U S A* **95**, 2498–2502.

Topp BG, Atkinson LL, Finegood DT (2007) Dynamics of insulin sensitivity, -cell function, and -cell mass during the development of diabetes in fa/fa rats. *Am J Physiol Endocrinol Metab*, **293**, E1730–E1735.